UC Irvine
UC Irvine Previously Published Works

Title
Molecular interference of fibrin's divalent polymerization mechanism enables modulation of multiscale material properties

Permalink
https://escholarship.org/uc/item/1hh3n7x2

Authors
Brown, Ashley C
Baker, Stephen R
Douglas, Alison M
et al.

Publication Date
2015-05-01

DOI
10.1016/j.biomaterials.2015.01.010

Copyright Information
This work is made available under the terms of a Creative Commons Attribution License, availalbe at https://creativecommons.org/licenses/by/4.0/

Peer reviewed

eScholarship.org Powered by the California Digital Library
University of California

Author Manuscript

Author Manuscript

Author Manuscript

Author Manuscript

HHS Public Access

Author manuscript

Biomaterials. Author manuscript; available in PMC 2016 May 01.

Published in final edited form as:

Biomaterials. 2015 May ; 49: 27–36. doi:10.1016/j.biomaterials.2015.01.010.

Molecular interference of fibrin's divalent polymerization mechanism enables modulation of multiscale material properties

Ashley C. Brown[1], **Stephen Baker**[2], **Alison Douglas**[3], **Mark Keating**[4], **Martha Alvarez-Elizondo**[4], **Elliot Botvinick**[4], **Martin Guthold**[2], and **Thomas H. Barker**[3,5]

[1]The School of Chemistry and Biochemistry, Georgia Institute of Technology, Atlanta, GA 30332

[2]Department of Physics, Wake Forest University, Winston-Salem, NC 27109

[3]The Wallace H. Coulter Department of Biomedical Engineering, Georgia Institute of Technology and Emory University, Atlanta GA 30332

[4]Beckman Laser Institute/Edwards Lifesciences Center for Advanced Cardiovascular Technology, University of California Irvine, Irvine, CA 92612

[5]The Parker H. Petit Institute for Bioengineering and Biosciences, Georgia Institute of Technology, Atlanta, GA 30332

Abstract

Protein based polymers provide an exciting and complex landscape for tunable natural biomaterials through modulation of molecular level interactions. Here we demonstrate the ability to modify protein polymer structural and mechanical properties at multiple length scales by molecular 'interference' of fibrin's native polymerization mechanism. We have previously reported that engagement of fibrin's polymerization '*hole b*', also known as 'b-pockets', through PEGylated complimentary '*knob B*' mimics can increase fibrin network porosity but also, somewhat paradoxically, increase network stiffness. Here, we explore the possible mechanistic underpinning of this phenomenon through characterization of the effects of *knob B*-fibrin interaction at multiple length scales from molecular to bulk polymer. Despite its weak monovalent binding affinity for fibrin, addition of both *knob B* and PEGylated *knob B* at concentrations near the binding coefficient, K_d, increased fibrin network porosity, consistent with the reported role of *knob B-hole b* interactions in promoting lateral growth of fibrin fibers. Addition of PEGylated *knob B* decreases the extensibility of single fibrin fibers at concentrations near its K_d but increases extensibility of fibers at concentrations above its K_d. The data suggest this bimodal behavior is due to the individual contributions *knob B*, which decreases fiber extensibility, and PEG, which increase fiber extensibility. Taken together with laser trap-based microrheological and bulk rheological analyses of fibrin polymers, our data strongly suggests that *hole b* engagement increases in single fiber stiffness that translates to higher storage moduli of fibrin polymers despite

Corresponding Author: Thomas H. Barker, Ph.D., Address: The Wallace H. Coulter Department of Biomedical Engineering at Georgia Tech and Emory University, 313 Ferst Drive, Suite 2108, Atlanta, GA 30332-0535, (404) 385-5039 – phone, (404) 894-4243 – fax, thomas.barker@bme.gatech.edu.

Publisher's Disclaimer: This is a PDF file of an unedited manuscript that has been accepted for publication. As a service to our customers we are providing this early version of the manuscript. The manuscript will undergo copyediting, typesetting, and review of the resulting proof before it is published in its final citable form. Please note that during the production process errors may be discovered which could affect the content, and all legal disclaimers that apply to the journal pertain.

Author Manuscript Author Manuscript Author Manuscript Author Manuscript

their increased porosity. These data point to possible strategies for tuning fibrin polymer mechanical properties through modulation of single fiber mechanics.

Introduction

Protein-based polymers, such as those derived from extracellular matrix proteins, are widely utilized as biomaterials due to their inherent biocompatibility and utility in a range of medical and tissue engineering applications. Protein-based polymers provide a complex landscape for modulation at the molecular level, through either chemical modification or modulation of specific molecular interactions with the protein. Modification of protein-based polymers at the molecular level can affect material properties at the bulk scale; such modifications could provide a rich parameter space for rational design of biomaterial properties. However, modification of proteins at this length scale has been underutilized in the fields of biomaterials and tissue engineering. Here we demonstrate the ability to modify protein polymer structural and mechanical properties over multiple length scales by simple molecular 'interference' of the polymerization mechanism of the widely utilized protein polymer, fibrin.

Fibrin is a hydrogel formed from the naturally derived blood clotting protein fibrinogen. It is widely utilized for a number of biomedical applications due to its intrinsic ability to provide cell instructive cues to direct regenerative processes as well as its ability to be degraded by natural proteolytic processes [1, 2]; it is the body's natural provisional wound-healing matrix. Fibrin monomer is derived from proteolytic cleavage of the soluble precursor molecule, fibrinogen, by the serine protease thrombin [3]. Upon activation fibrin monomers self-assemble through '*knob-hole*' interactions to form an insoluble network [4, 5]. Fibrin network properties, both structural and mechanical, are influenced by the polymerization conditions including initial fibrinogen and thrombin concentrations, buffer ionic strength, pH, and calcium concentration [6–8]. Commercially available fibrin products utilize exceptionally high concentrations of fibrinogen and thrombin to achieve fast polymerization and impart mechanical integrity to the constructs [2]. However, typical fibrinogen concentrations of these products (30–100 mg/mL) are an order of magnitude higher than physiological circulating concentrations (~3 mg/mL). Despite their attractive physical properties, these high concentrations of fibrinogen and thrombin result in fibrin networks that lack the porosity necessary to facilitate optimal cellular infiltration [9]. There is interest, therefore, in modifying fibrin matrices to allow for increased network porosity while maintaining fast polymerization dynamics and mechanical integrity. To that end our group has previously created synthetic peptides variants that engage native fibrin polymerization mechanisms to altered network properties [10, 11].

Fibrinogen is comprised of two identical subunits, which each contain three chains known as the Aα, Bβ and γ chains. The 'A' and 'B' designation refer to N-terminal 16- and 14-amino acid peptides, respectively, which are released by thrombin cleavage (activation), leading to exposure of peptide sequences at the N termini of the α and β chains, termed knobs *A* and *B*, respectively. *Knobs A* and *B* interact with complementary *holes a* and *b* located in the two distal 'D domains' of the γ and β chains on neighboring fibrinogen molecules. Because *holes*

Author Manuscript Author Manuscript Author Manuscript Author Manuscript

a and *b* do not require enzymatic cleavage to bind to their respective knob peptides, synthetic *knob* peptides have been utilized to modify fibrin network architecture for tissue engineering and/or drug delivery applications. Our group has created a variety of *knob* mimic constructs including *knob-A*-protein constructs [10], PEGylated *knobs A* and *B* [11, 12] and *knob A* modified elastin like peptide micelles [13] and we have characterized their effect on fibrin properties such as polymerization, degradation, mechanical properties and network structure.

The N-terminal Gly-Pro-Arg (GPR) motif found on the α chain is the minimum *knob A* sequence required to facilitate binding to a complimentary *hole a* located in the γ chains [14, 15]. The human *knob B* motif is comprised of the N-terminal Gly-His-Arg-Pro (GHRP) motif and is complementary to *hole b* located in the β chains [16]. *A:a* interactions appear to be the primary contributor to fibrin polymerization; polymerization is inhibited in the presence of high concentrations of a synthetic *knob A* of the sequence Gly-Pro-Arg-Pro (GPRP) [15]. *B:b* interactions appear to be less crucial in primary fibrin formation and clots can be formed in the absence of *knob B* exposure [4, 17]. There is some debate over the physiological relevance and specific functional role of *B:b* interactions, however our and others' studies suggest that *B:b* interactions promote lateral aggregation and play a role in determining clot stability and susceptibility to degradation [11, 18].

Because *B:b* interactions are not essential to fibrin network formation, modification of fibrin network properties through synthetic *knob B* mimics is perhaps more attractive than through *knob A* mimics because one can alter properties without adversely affecting primary polymerization. Despite a few reports of *knob-hole* cross-reactivity, the *knob B* mimic derived from chicken (AHRP) has previously been demonstrated to only bind to *hole B* [19, 20]. Further studies with the bovine *knob B* mimic (GHRPY) demonstrated that the Tyr5 residue contributes to an altered molecular packing of fibrinogen molecules that leads to altered network structure and delayed fibrinolysis [18, 21]. We recently utilized a PEGylated *knob B* mimic, AHRPYAAC, to combine the *knob B* specificity of the AHRP sequence with the altered molecular packing of fibrinogen molecules of XHRPY sequences [11]. This PEGylated- AHRPYAAC construct enhanced the porosity of the fibrin network, decreased susceptibility to degradation and increased the complex modulus (G^*). These prior studies were performed at a 1:1 molar ratio of fibrinogen:knob mimic to allow for direct comparison with equimolar concentration of PEGylated *knob A* mimics, however the reaction kinetics of *A:a* and *B:b* interactions vary greatly. Furthermore, the initial release of *knob A* by thrombin cleavage is significantly faster than the exposure of *knob B*, but as polymerization proceeds, the rate of *knob B* exposure increases, a process thought to be driven by conformation changes [22]. Utilizing *knob B* mimics at concentrations which are close to its K_d would allow for more robust control over fibrin network properties mediated by pre-engagement of the *hole b*.

We hypothesized that the effect of AHRPYAAC-PEG on fibrin network properties would be more pronounced at concentrations near the K_d of *B:b* interactions. Here, we first characterize the binding kinetics of free and PEGylated *knob B* mimics to fibrinogen fragment D and then investigate the effect of these synthetic *knobs* on fibrin network properties at concentrations below, near and above the K_d. In these studies, we characterize

Author Manuscript Author Manuscript Author Manuscript Author Manuscript

the effect of PEGylated *knob B* on clot properties at multiple length scales by analyzing events at the molecular, nano- and micro- scale.

Materials and Methods

Preparation and characterization of PEGylated knobs

Knob B and non-binding control cysteine-terminated peptides, AHRPYAAC and GPSPFPAC respectively, were custom-ordered from Genscript (Piscataway, NJ) in lyophilized form. Peptides were conjugated to 5 kDa maleimide-PEG (JenKem Technology, Allen, TX) by reacting components at a 10:1 peptide to PEG molar ratio in 100 mM phosphate buffer pH 7.2, 150 mM NaCl, 10mM EDTA for four hours at room temperature. Excess unconjugated peptide was removed from the conjugated product through dialysis overnight into deionized water utilizing 2 kD molecular weight cutoff membranes (Slidalyzer, Thermo Fisher Scientific). The product was aliquoted, lyophilized and quantified. PEG and peptide concentrations were quantified through a barium chloride PEG assay and the CBQCA amine assay, respectively. Briefly, the barium chloride assay for PEG quantitation was based on the method of Sims and Snape and modified for a 96-well plate format [23]. 80 μL of sample was incubated with 20 μL of barium chloride solution (5% in 1 M HCL). 10 μL of 0.1 N iodine solution was then added to each well and absorbance was measured at 535 nm using a plate reader. PEG concentration was calculated through the use of a standard curve generated with unconjugated 5 kD PEG. Peptide concentration was then determined using the CBQCA assay kit (Invitrogen, Carlsbad, CA) according to manufacture specifications using unconjugated AHRPYAAC or GPSPFPAC peptides to generate standard curves.

Preparation of fibrinogen fragment D

Human fibrinogen (FIB 3, Enzyme Research Laboratories (ERL)) at 2 mg/mL was digested with 0.1 U/mL human plasmin (ERL) in HEPES (N-2-hydroxyethylpiperazine-N′-2-ethanesulfonic acid) $CaCl_2$ buffer (150mM NaCl, 5mM $CaCl_2$, 25mM HEPES; pH 7.4) overnight at room temperature. Fragment D was isolated by incubating the plasmin-digested fibrinogen with GPRPAA beads at room temperature for 30 minutes, with occasional agitation [24, 25]. The unbound proteins and protein fragments were removed with excessive washing with HEPES + $CaCl_2$ buffer. Fragment D was eluted with 1M sodium bromide and 50mM sodium acetate (pH 5.3). Eluted samples were pooled together and exchanged back into HEPES + $CaCl_2$ buffer with a centrifugal filter (molecular weight cutoff, 10,000 Da). Fragment D was verified by sodium dodecyl sulfate–polyacrylamide gel electrophoresis and stored at −80°C until use.

Surface Plasmon Resonance

The Biacore 2000 (Biacore Lifesciences, GE Healthcare) was used to investigate kinetic binding constants (k_a and k_d) of *knob* peptide variants for fibrinogen Fragment D, which contains the polymerization *holes*. Briefly, Fragment D was covalently immobilized to gold-coated SPR sensor chips via self-assembled monolayer surface chemistry to generate a nonfouling surface with a controlled density of reactive carboxylic acid groups. Mixed self-assembled monolayers were generated on gold-coated chips by incubating with a 1-mM

Author Manuscript Author Manuscript Author Manuscript Author Manuscript

mixture of tri(ethylene glycol)–terminated alkanethiols (HS-(CH2)11–(OCH2CH2)3–OH; ProChimia) and carboxylic acid– terminated alkanethiols (HS-(CH2)11–(OCH2CH2)6–OCH2COOH) overnight [25]. On loading the senor chip into the Biacore 2000, the carboxylic acid–terminated alkanethiols in all 4 flow cells was activated by flowing 200 mM 1-ethyl-3-(3-dimethylaminopropyl) carbodiimide (Sigma- Aldrich) and 50 mM N-hydroxysuccinimide (Sigma-Aldrich; 5 μL/minute for 10 minutes). Immediately after activation, Fragment D was immobilized in 3 flow cells (5 μL/minute for 10 minutes) to achieve approximately 1500 resonance units (1 resonance unit ~1 pg/mm^2). Unreacted N-hydroxysuccinimide groups were quenched in all 4 flow cells (3 sample cells and 1 reference cell) with 20 mM ethanolamine (10 μL/minute for 10 minutes). On stabilization of the baseline signal, kinetic binding experiments were run in duplicate with the peptide variants as the flow analytes. Five different concentrations for each peptide (ranging from 5 μM to 1.5 mM) were flowed at 25 μL/minute for 4 minutes immediately followed by a 5-minute dissociation phase. Between each run, the surface was regenerated with 1 M sodium bromide and 50 mM sodium acetate (pH 6.0).

SPR analysis and evaluation

SPR sensorgrams were analyzed with the aid of Scrubber 2 and ClampXP software (Center for Biomolecular Interactions Analysis, University of Utah) [26–28]. Sensorgrams with abnormalities (ie, baseline drift, air spikes, or irregular deviations) were excluded from analysis. Reference cell responses were subtracted from corresponding active response curves. Double-referenced curves were acquired by further subtracting the reference cell blank buffer injections from each reference subtracted response curve. All double-referenced curves were normalized by the molecular weight of each peptide and multiplied by 1000 to account for minor variations in response because of molecular weight. The resulting curves were then analyzed and fitted to the kinetic models. Kinetic modeling and simulations were performed with ClampXP software with the Langmuir 1:1 model or the heterogeneous ligand model; globally fitted parameters were determined for each kinetic dataset per peptide. Equilibrium binding constants were calculated from fitted kinetic constants. Goodness of fit for each model was determined by evaluating the residual plots and residual sum of squares.

Confocal Microscopy

Clot structure was analyzed using fluorescence confocal microscopy. Fibrin clots were prepared with a final fibrinogen concentration (FIB 3, ERL) of 1 mg/mL and 0.25 U/mL thrombin (human α-thrombin, ERL) in the presence or absence of various concentrations of free peptides or PEGylated peptides (1 mM, 250 μM and 100 μM) and examined using confocal microscopy (63x oil immersion objective, NA 1.4; Zeiss 510 VIS). These concentrations of peptides were chosen because they represented concentrations above, near and below the K_d values calculated for PEGylated *knob B* binding to fibrinogen fragment D. To allow for visualization of the fibrin matrix, Alexa Fluor 647-labeled fibrinogen was utilized for these assays. Clots were formed directly on a glass slide, overlaid with a coverslip and allowed to polymerize for an hour prior to imaging.

Author Manuscript Author Manuscript Author Manuscript Author Manuscript

Clot Polymerization Assays

Fibrin polymerization dynamics were observed in the presence of various concentrations (1 mM, 250 μM and 100 μM) of free and PEGylated *knob B* and control peptide. Clots were formed in 25 mM HEPES, 150 mM NaCl, pH 7.4 with final fibrinogen, thrombin and $CaCl_2$ concentrations of 1 mg/mL, 0.25 U/mL and 5 mM, respectively. Polymerization was monitored by real time analysis of clot turbidity through measuring A350 every minute for one hour using a plate reader (BioTek Synergy H4, Winooski, VT). Baseline absorbance values were subtracted from each reading and polymerization curves were analyzed to determine various parameters including final turbidity, half-max polymerization time and rate of polymerization. Half-max polymerization time corresponds to the time required to reach half of the maximum turbidity value. Following the one-hour polymerization phase, the amount of unclotted protein was determined by analyzing the clot liquor for total protein using the Quant-it protein assay (Invitrogen). Percent clottable protein was determined by comparing each experimental sample to negative control fibrinogen only samples.

Microrheology of fibrin clots

Local material response functions within hydrogels were measured by active microrheology (AMR) as previously described [29, 30]. Fibrin gels were polymerized as described in previous sections but with the addition of 2 μm microbeads added to the unpolymerized solution at a concentration of 1 mg/mL. A set of microbeads were chosen at random for active microrheology. Briefly, a microbead is oscillated by optical tweezers (1064 nm laser microbeam) steered by galvanometer mirrors. A detection laser microbeam (785nm) not steered by mirrors is focused onto the microbead, which deflects the detection beam as the microbead oscillates in position. Detection beam deflection is measured by a quadrant photodiode that outputs analog signals related to the absolute position of the bead. The optical trapping beam was oscillated sinusoidally with amplitude of 60 nm at frequencies 10, 20, 50, 75, and 100 Hz. Local material properties, including the complex shear modulus G* are computed from the amplitude-phase response of each microbead relative to the laser. G* is decomposed into the storage and loss moduli, G' and G'' respectively [31].

Bulk Rheology

Oscillatory rheology was performed on the various fibrin constructs using a cone-plate rheometer (Anton Paar, Graz, Austria) with a 25 mm diameter tool attachment. Clots were formulated as previously described and allowed to polymerize in contact with the tool for one hour prior to measurements. Frequency sweeps were performed over a frequency range from 0.01 Hz to 10 Hz at 0.1% strain to obtain storage and loss moduli. Average storage moduli were calculated from the average value over the frequency range for three different gel constructs. Data is represented as mean +/− SEM.

Formation of Fibrin Fibers for Single Fiber Experiments

Mimetic *knob B* (AHRPYAAC) was added to a fibrinogen solution in HEPES buffer (140 mM NaCl, 10 mM HEPES, 5 mM CaCl2, pH 7.4) and allowed to incubate at 37°C for 15 min. After incubation, Human alpha Thrombin (ERL) and Human Factor XIII (FXIII) (ERL) were added to the solution and a clot was allowed to form on striated substrates made

Author Manuscript Author Manuscript Author Manuscript Author Manuscript

from optical glue, as described previously, for 75 min [32]. Final concentrations of mimetic *knob B* for different samples were 1 mM, 250 μM, and 100 μM respectively. The final concentration of fibrinogen, thrombin, and FXIII were 3.2 μM (1.09 mg/ml), 0.3 NIH u/ml, and 9.00 Loewy u/ml respectively. Clots were also formed using PEGylated *knob B* with final concentrations of 1 mM, 250 μM, and 100 μM as described above. Control clots were formed from a fibrinogen solution and 5 kDa PEG with final concentrations of PEG being 1 mM, 250 μM, and 100 μM as before. After clots were formed, fibers were labeled with 24 nm yellow-green carboxyl fluorescent beads (Invitrogen, Fluospheres, Carlsbad, CA) diluted 1/100 in fibrin buffer-2 (10mM HEPES, 140mM NaCl, pH 7.4). A 200 μl drop was added directly to the clot on the cover slide and allowed to bind to the fibers for 10 min. The slide was then rinsed and stored with HEPES buffer.

Combined Atomic Force Microscopy (AFM)/Fluorescent Microscopy

Fibrin fiber manipulations were performed using a combined atomic force/fluorescent microscopy technique [32, 33]. The AFM (Topometrix Explorer, Veeco Instruments, Woodbury, NY) rests on a custom-made stage on top of an inverted microscope (Zeiss Axiovert 200, Göttingen, Germany). The cover slide with the fibrin sample is sandwiched between the AFM and the fluorescent microscope. The stage is designed to allow for independent movement of the fibrin sample, objective, and AFM cantilever. Fluorescence images were captured using a Hamamatsu EM-CCD C9100 Camera (Hamamatsu Photonics KK, Japan) and IPLab software (Scanalytics, Fairfax, VA). The AFM cantilever tip (CSC38/AlBS, force constant 0.03–0.08 N/m, MikroMasch, Wilson, OR) was placed between two of the ridges in the striated substrate, next to a fiber for manipulation. The cantilever tip, controlled by nanoManipulator software (3rd Tech, Chapel Hill, NC) was then laterally moved to stretch a single fiber at a rate of 305 nm/s. The elapsed time, tip travel distance, and left-right photodiode signal were recorded by the nanoManipulator software.

Force and Strain Calculations

The force applied to single fibrin fibers and single fiber strain were calculated as previously reported [32]. The lateral force spring constant K_c, is determined from cantilever beam mechanics, $K_C = \frac{Ewt^3}{6l^2(h+t/2)} \cdot S_n$, where E is the Young's modulus of silicon (1.69×10^{11} N/m^2), w, t, and l are the cantilever width, thickness and length respectively, S_n is the normal sensor response of the cantilever, and h is the height of the tip. Using this and the left-right photodiode signal, I_l, we can determine the lateral force using $F_l = K_C \cdot I_l$. The height of the tip and length and width of the cantilever were found using the optical microscope. The thickness was calculated using the resonance frequency of the cantilever, $f = 0.276 \cdot \sqrt{\frac{Ewt^3}{\rho(\pi \cdot h^3 \cdot l^3 + 2.832 \cdot w \cdot t \cdot l^4)}}$, where ρ is the density of silicon (2330 kg/m^3). The force applied to the fiber, $F_{fiber} = \frac{F_l}{2\sin\beta}$, was found using the lateral force measured by the AFM tip, F_l, and $\beta = \arctan\frac{s}{L_{initial}}$ found from Figure 6B, where s is the distance the tip traveled, recorded by nanoManipulator and $L_{initial}$ is the initial length of the fiber. The strain

Author Manuscript Author Manuscript Author Manuscript Author Manuscript

of each individual fiber was calculated from $\varepsilon = \frac{L' - L_{initial}}{L_{initial}}$, where L' is the length of the stretched fiber and $L_{initial}$ is the initial length of the fiber.

Statistical Analysis

All statistical analyses were performed with Prism software program (GraphPad, San Diego CA). Data was analyzed using a one way analysis of variance (ANOVA) using a Tukey or Scheffe posthoc test at a 95% confidence interval.

Results

Binding kinetics

The binding capacities of *knob B* peptide, AHRPYAAC, non-binding peptide, GPSPFPAC, and their respective PEGylated peptides to fragment D were determined through SPR. Experimental SPR curves were fit to a Langmuir 1:1 model or a 2-site model to determine the association and dissociation rates (k_a, k_d, respectively) for each peptide variant. Goodness of Fit was analyzed by the residual sum of squares (RSS), which characterizes the difference between the experiment values and the fitted curves. A lower RSS corresponds to a better fit, and in general, this value should be below 10% of the maximum binding response. The RSS was evaluated for all *knob* peptide variants fit to both the Langmuir 1:1 model as well as the 2-site model. *Knob B* native peptides and their PEGylated counterparts best fit a 2-site model, while the non-binding control only converged when fit to the Langmuir 1:1 model. Binding to fragment D was only observed for the native non-binding peptide and the PEGylated version at high (mM) concentrations, which is likely due to nonspecific interactions. Previous reports characterizing the affinity of *knob A* for fragment D also reported a 2-site binding model [25], presumably because *knob A* binds both *hole a and hole b*. The binding affinities of the *knob B* have not been previously reported, however, *knob B* is thought to only bind *hole b*. Examination of the fitted parameters for the 2-site model of *knob B* demonstrate one higher and one lower affinity interaction, with these values being two orders of magnitude apart for the PEGylated *knob B*. The higher affinity reaction is assumed to be the specific interaction of *knob B* and *hole b*, whereas the lower affinity reaction likely corresponds to nonspecific binding, as we have previously reported [25]. The experimental sensograms and their respective best fits are shown below in Figure 1. The fitted parameters (k_a, k_d) for each *knob* peptide variant are displayed in Supplemental Table 1. K_{d1}, again assumed to be the specific interaction of *knob B* and *hole b*, was found to be 31 μM for free *knob B* peptide and 57 μM for the PEGylated *knob B*. The lower affinity K_{d2}, likely corresponding to nonspecific binding, was found to be 80 μM for free *knob B* peptide and 1750 μM for the PEGylated *knob B*. The calculated K_d for the nonbinding control peptides and their PEGylated counterpart were found to be 181 and 290 μM, respectively. These results indicate that, at a minimum, micromolar concentrations of PEGylated *knob B* peptides are required to observe binding to fibrinogen. We therefore utilized peptide concentrations ranging from 100 μM – 1 mM for subsequent studies.

Author Manuscript Author Manuscript Author Manuscript Author Manuscript

Confocal Microscopy

Fibrin clots were polymerized in the presence of free or PEGylated *knob B* peptide or the non-binding control and examined using confocal microscopy. Inclusion of free or PEGylated *knob B* peptide greatly altered fibrin network structure, resulting in thicker fibers and an increased porosity (Figure 2) in a concentration dependent manner. The addition of free non-binding peptide had minimal effect on clot structure, while the PEGylated non-binding peptide resulted in slight modifications of clot structure. Clots formed in the presence of the PEGylated non-binding peptides were found to have slightly more porous networks and thicker fibers than those observed in control clots. These differences highlight the different effects of *knob B* and PEG in alterations of clot structure.

Clot Polymerization Assays

Fibrin polymerization dynamics were analyzed in the presence of free or PEGylated *knob B* peptide, non-binding control peptide or free PEG by monitoring turbidity every minute for 1 hour. Final turbidity was increased in the presence of free PEG at all concentrations tested while 1 mM concentrations of free 'B' peptide decreased turbidity (Figure 3, Supplemental Figure 1). It should be noted that confocal images demonstrate that the structures observed in the presence of free and PEGylated 'B' peptide, as well as free PEG, are extremely heterogeneous; turbidity measurements average over the entire structure and therefore these final turbidity measurements are somewhat difficult to interpret. Nonetheless, monitoring turbidity during polymerization does allow for direct monitoring of polymerization dynamics including polymerization rates. It was found that free *knob B* peptide increased the rate of polymerization at all concentrations tested. Interestingly, PEGylated *knob B*, along with free and PEGylated control peptides and free PEG, did not significantly alter polymerization rates except at 1 mM concentrations (Figure 3C). This increase could potentially be due to a molecular crowding effect due to high concentrations of PEG leading to a concentration of clotting factors. Following completion of polymerization, percent clottable protein was determined by measuring the protein content of the clot liquor and comparing values to fibrinogen only (no thrombin) controls (Figure 4). It was found that the presence of both free and PEGylated *knob B* peptide significantly decreased percent clottability ($p<0.001$) compared to the fibrin only control in a dose dependent manner. Clots formed in the presence of 1 mM free or PEGylated *knob B* peptide were found to be only 26% or 34% clottable compared to fibrin controls which were 92% clottable. Polymerization in the presence of free PEG or GPSPFPAC-PEG was significantly inhibited at 1mM concentrations, and clots formed in the presence of these compounds were found to be 77% and 79% clottable, respectively. Polymerization was not significantly affected by the presence of free GPSPFPAC peptide; clots were found to be between 88% and 92% clottable for all concentrations tested.

Micro and Bulk Rheology

We characterized storage modulus of fibrin clots at both the micro and macro scales utilizing AMR and bulk rheology, respectively. For all conditions, G' was not dependent on the frequency of oscillation (for the range tested) and we report the average value across frequencies. AMR results demonstrate that AHRP-PEG peptides increase storage modulus

Author Manuscript Author Manuscript Author Manuscript Author Manuscript

(G′) in a dose dependent manner compared to control and at 1 mM concentrations, G′ is more than doubled and is significantly different ($p<0.05$) than control samples. An increase in storage modulus was also observed in the presence of free *knob B* peptide and free PEG, however these responses were muted in comparison and were not significantly different than control samples, indicating that the increased storage modulus has an additive effect. Interestingly, an initial spike in G′ was also observed upon addition of GPSPAAC-PEG samples compared to fibrin only controls ($p<0.05$) but G′ decreased with subsequent increases in GPSPAAC-PEG concentrations and was not significantly different than control samples. No significant differences in storage moduli were observed through bulk rheology analysis under any of the conditions tested.

Single Fiber Breaking Strain

We determined the breaking strain for individual fibrin fibers as is described previously [32]. Briefly, breaking strain was determined by stretching individual fibers attached at adjacent parallel ridges until they broke as can be seen in Figure 6. All fibers were stretched at a constant a rate of 305 nm/s. Figure 6D shows force strain curves for single fiber manipulations at low (100 μM) and high (1 mM) *knob B* concentrations while also showing that as the force applied to the AFM tip increased the force required to stretch the fibers also increased. Average single fiber breaking strains for 1 mM, 250 μM, and 100 μM concentrations of mimetic *knob B* (AHRPYAAC, AHRPYAAC-PEG) and free PEG as well as unmodified fibrin are shown in Figure 6E. At a 1 mM concentration of AHRPYAAC the breaking strain for individual fibers decreases by 78% when compared to unmodified fibrin fibers and slowly returned closer to the breaking strain for unmodified fibrin fibers as the concentration is lowered to 250 μM and then 100 μM. 1 mM concentrations of AHRPYAAC-PEG have an average breaking strain of 202%, 20% higher than the average breaking strain for unmodified fibrin fibers. At concentrations of 250 μM and 100 μM the average breaking strain drops to 164% and 171% respectively. For samples where PEG was added to a solution of fibrinogen prior to polymerization into fibrin, we see that the average breaking strain drops from 215% at 1 mM to 195% at 250 μM and finally to 167% at 100 μM.

Discussion

Incorporation of both free and PEGylated synthetic *knob B* peptides significantly alter clot architecture, polymerization kinetics and mechanical properties. The engagement of *hole b* by synthetic peptides leads to the formation of a heterogeneous network displaying regions of dense fibrin interspersed among large pores. These changes are accompanied by a concentration dependent decrease in percent clottability, indicating less available protein is incorporated into the resulting clot, a result that is consistent with the highly porous nature of clots formed in the presence of both free *knob B* peptide and PEGylated *knob B*. Interestingly, free *knob B* peptides also significantly increase the rate of polymerization. Native *knob B* is thought to be exposed (via thrombin cleavage and release of the N-terminal fibrinopeptide B) at a slower rate than *knob A*, however engagement of *hole b* by *knob B* is thought to elicit a conformation change in fibrinogen which enhances further *knob:hole* interactions [11, 22, 34]. Our results that pre-engagement of *hole b* by synthetic *knob B*

Author Manuscript Author Manuscript Author Manuscript Author Manuscript

peptides leads to enhanced rates of polymerization, could be due to this previously described *knob B* induced confirmation change.

Despite the increase in porosity and decreased clottability associated with engagement of *hole b*, these networks display increased stiffness at the micromechanical level. These results are enhanced greatly when the *knob B* peptide is PEGylated. We hypothesize that the lack of statistically significant differences in the bulk rheological measurements at the concentrations tested is due to the heterogeneous nature of the clots where slight differences in microarchitecture are averaged. For example, the combination of increased fiber stiffness with increased porosity as seen with the addition of PEGylated *knob B* could have competing effects on the storage modulus resulting in no change from the control group. AMR analysis indicates that the effect of PEG and *knob B* appear to be additive for enhancing storage modulus. However, free PEG and *knob B* peptide have opposite effects on fiber mechanics. Breaking strain decreases (fibers become less extensible) in the presence of free *knob B* peptide but also increases in the presence of free PEG, compared to control fibrin only fibers. Interestingly, the addition of PEGylated *knob B* decreases the extensibility of fibers at concentrations near its K_d but increase extensibility of fibers at concentrations above its K_d, indicating that the effects of PEG may dominate at higher concentrations.

It is well known that *knob A:hole a* interactions occur with higher affinity compared to *knob B:hole b* interactions, and are approximately six times stronger [35, 36]. The functional consequences of *knob B:hole b* interactions have been a topic of debate in the fibrin field. However, our data demonstrate that either free or PEGylated *knob B* peptides, when utilized at concentrations near or above their K_d concentration for Fragment D, significantly influence clot polymerization dynamics as well as structural and mechanical properties. While *knob B:hole b* interactions are not required for clot formation, they do influence clotting dynamics and, based on the current study, fibrin fiber and clot architecture. These data provide insight into the role of *knob B:hole b* interactions in clot formation.

Clot modifications via *knob B* molecular interference of polymerization may have interesting and advantageous properties for biomedical applications. Fibrin is a widely used biomaterial for tissue sealants and tissue engineering scaffolds; however, current commercial formulations lack the balance between mechanical properties and porosity required to achieve optimal handleability for clinical applications while also allowing for cell infiltration. The ability to create clots with increased porosity in conjunction with altered mechanical properties, as we have demonstrated here in the presence of *knob B* peptides, might be advantageous for addressing these current limitations.

Conclusion

Engagement of the fibrinogen *hole b* by synthetic *knob B*, either synthetic or PEGylated, significantly alters clot structure, polymerization dynamics and mechanical properties. Clots formed in the presence of synthetic *knob B* peptides are considerably more porous, polymerize faster, display increased G' at the microscale and are comprised of fibers with increased elastic modulus but decreased extensibility compared to control clots. PEGylation of these *knob*s display similar features, however, the effect of PEG can be observed in

Author Manuscript Author Manuscript Author Manuscript Author Manuscript

increased G′ as measured by AMR and increased fiber extensibility at higher concentrations. These data provide new insights into the kinetics of *knob B:hole b* interactions and their role in fibrin polymerization and clot structure. These data also demonstrate the effect of PEGylation on modification of *knob B:hole b* interactions and resulting further alterations to clot properties. PEGylated synthetic *knob B* could be utilized for targeting purposes for drug delivery or modification of fibrin networks for tissue engineering purposes.

Supplementary Material

Refer to Web version on PubMed Central for supplementary material.

Acknowledgments

Funding sources: NIH (R21-EB008463 and 1R01EB011566) and the Center for Advanced Bioengineering for Soldier Survivability (DoD W81XWH1110306) to THB, American Heart Association Postdoctoral Fellowship to ACB, the Wake Forest University Translational Science Center (U01078, U01508), and the Wake Forest University Center for Molecular Communication and Signaling (U01057)

References

1. Janmey PA, Winer JP, Weisel JW. Fibrin gels and their clinical and bioengineering applications. Journal of the Royal Society, Interface/the Royal Society. 2009; 6:1–10.
2. James Ferguson, SN.; Redl, Heinz. Fibrin: The Very First Biomimetic Glue — Still a Great Tool. In: Byern, J.; Grunwald, Ingo, editors. Biological Adhesive Systems. Springer; Vienna: 2010. p. 225-36.
3. Mosesson MW, Siebenlist KR, Meh DA. The structure and biological features of fibrinogen and fibrin. Annals of the New York Academy of Sciences. 2001; 936:11–30. [PubMed: 11460466]
4. Furlan M, Seelich T, Beck EA. Clottability and cross-linking reactivity of fibrin(ogen) following differential release of fibrinopeptides A and B. Thrombosis and haemostasis. 1976; 36:582–92. [PubMed: 14415]
5. Litvinov RI, Gorkun OV, Owen SF, Shuman H, Weisel JW. Polymerization of fibrin: specificity, strength, and stability of knob-hole interactions studied at the single-molecule level. Blood. 2005; 106:2944–51. [PubMed: 15998829]
6. Potier ENJ, Sprecher C, Ito K. Influencing biophysical properties of fibrin with buffer solutions. J Mater Sci. 2010; 45:2494–503.
7. Duong H, Wu B, Tawil B. Modulation of 3D fibrin matrix stiffness by intrinsic fibrinogen-thrombin compositions and by extrinsic cellular activity. Tissue engineering Part A. 2009; 15:1865–76. [PubMed: 19309239]
8. Ryan EA, Mockros LF, Weisel JW, Lorand L. Structural origins of fibrin clot rheology. Biophysical journal. 1999; 77:2813–26. [PubMed: 10545379]
9. Schmoekel HG, Weber FE, Schense JC, Gratz KW, Schawalder P, Hubbell JA. Bone repair with a form of BMP-2 engineered for incorporation into fibrin cell ingrowth matrices. Biotechnology and bioengineering. 2005; 89:253–62. [PubMed: 15619323]
10. Soon AS, Stabenfeldt SE, Brown WE, Barker TH. Engineering fibrin matrices: the engagement of polymerization pockets through fibrin knob technology for the delivery and retention of therapeutic proteins. Biomaterials. 2010; 31:1944–54. [PubMed: 19914710]
11. Stabenfeldt SE, Gourley M, Krishnan L, Hoying JB, Barker TH. Engineering fibrin polymers through engagement of alternative polymerization mechanisms. Biomaterials. 2012; 33:535–44. [PubMed: 22018389]
12. Soon AS, Lee CS, Barker TH. Modulation of fibrin matrix properties via knob:hole affinity interactions using peptide-PEG conjugates. Biomaterials. 2011; 32:4406–14. [PubMed: 21435714]
13. Soon AS, Smith MH, Herman ES, Lyon LA, Barker TH. Development of Self-Assembling Mixed Protein Micelles with Temperature-Modulated Avidities. Advanced healthcare materials. 2013

Author Manuscript Author Manuscript Author Manuscript Author Manuscript

14. Laudano AP, Doolittle RF. Synthetic peptide derivatives that bind to fibrinogen and prevent the polymerization of fibrin monomers. Proceedings of the National Academy of Sciences of the United States of America. 1978; 75:3085–9. [PubMed: 277910]
15. Laudano AP, Doolittle RF. Studies on synthetic peptides that bind to fibrinogen and prevent fibrin polymerization. Structural requirements, number of binding sites, and species differences. Biochemistry. 1980; 19:1013–9. [PubMed: 7356959]
16. Doolittle RF, Pandi L. Probing the beta-chain hole of fibrinogen with synthetic peptides that differ at their amino termini. Biochemistry. 2007; 46:10033–8. [PubMed: 17688324]
17. Weisel JW. Fibrin assembly. Lateral aggregation and the role of the two pairs of fibrinopeptides. Biophysical journal. 1986; 50:1079–93. [PubMed: 3801570]
18. Doolittle RF, Pandi L. Binding of synthetic B knobs to fibrinogen changes the character of fibrin and inhibits its ability to activate tissue plasminogen activator and its destruction by plasmin. Biochemistry. 2006; 45:2657–67. [PubMed: 16489759]
19. Weissbach L, Oddoux C, Procyk R, Grieninger G. The beta chain of chicken fibrinogen contains an atypical thrombin cleavage site. Biochemistry. 1991; 30:3290–4. [PubMed: 2009266]
20. Doolittle RF, Chen A, Pandi L. Differences in binding specificity for the homologous gamma- and beta-chain “holes” on fibrinogen: exclusive binding of Ala- His-Arg-Pro-amide by the beta-chain hole. Biochemistry. 2006; 45:13962–9. [PubMed: 17115691]
21. Pandi L, Kollman JM, Lopez-Lira F, Burrows JM, Riley M, Doolittle RF. Two families of synthetic peptides that enhance fibrin turbidity and delay fibrinolysis by different mechanisms. Biochemistry. 2009; 48:7201–8. [PubMed: 19588915]
22. Lewis SD, Shields PP, Shafer JA. Characterization of the kinetic pathway for liberation of fibrinopeptides during assembly of fibrin. The Journal of biological chemistry. 1985; 260:10192–9. [PubMed: 4019507]
23. Gong XW, Wei DZ, He ML, Xiong YC. Discarded free PEG-based assay for obtaining the modification extent of pegylated proteins. Talanta. 2007; 71:381–4. [PubMed: 19071315]
24. Kostelansky MS, Betts L, Gorkun OV, Lord ST. 2.8 angstrom crystal structures of recombinant fibrinogen fragment D with and without two peptide ligands: GHRP binding to the “b” site disrupts its nearby calcium-binding site. Biochemistry. 2002; 41:12124–32. [PubMed: 12356313]
25. Stabenfeldt SE, Gossett JJ, Barker TH. Building better fibrin knob mimics: an investigation of synthetic fibrin knob peptide structures in solution and their dynamic binding with fibrinogen/fibrin holes. Blood. 2010; 116:1352–9. [PubMed: 20484082]
26. Morton TA, Myszka DG. Kinetic analysis of macromolecular interactions using surface plasmon resonance biosensors. Method Enzymol. 1998; 295:268.
27. Myszka DG. Kinetic analysis of macromolecular interactions using surface plasmon resonance biosensors. Curr Opin Biotech. 1997; 8:50–7. [PubMed: 9013659]
28. Morton TA, Myszka DG, Chaiken IM. Interpreting Complex Binding-Kinetics from Optical Biosensors - a Comparison of Analysis by Linearization, the Integrated Rate-Equation, and Numerical-Integration. Anal Biochem. 1995; 227:176–85. [PubMed: 7668379]
29. Kotlarchyk MA, Shreim SG, Alvarez-Elizondo MB, Estrada LC, Singh R, Valdevit L, et al. Concentration independent modulation of local micromechanics in a fibrin gel. PloS one. 2011; 6:e20201. [PubMed: 21629793]
30. Kniazeva E, Weidling JW, Singh R, ELB, Digman MA, Gratton E, et al. Quantification of local matrix deformations and mechanical properties during capillary morphogenesis in 3D. Integr Biol. 2012; 4:331–9.
31. Brau RR, Ferrer JM, Lee H, Castro CE, Tam BK, Tarsa PB, et al. Passive and active microrheology with optical tweezers. J Opt A: Pure Appl Opt. 2007:9.
32. Liu W, Carlisle CR, Sparks EA, Guthold M. The mechanical properties of single fibrin fibers. Journal of thrombosis and haemostasis: JTH. 2010; 8:1030–6. [PubMed: 20088938]
33. Baker S, Sigley J, Carlisle CR, Stitzel J, Berry J, Bonin K, et al. The Mechanical Properties of Dry, Electrospun Fibrinogen Fibers. Materials science & engineering C, Materials for biological applications. 2012; 32:215–21.

Author Manuscript Author Manuscript Author Manuscript Author Manuscript

34. Litvinov RI, Gorkun OV, Galanakis DK, Yakovlev S, Medved L, Shuman H, et al. Polymerization of fibrin: Direct observation and quantification of individual B:b knob-hole interactions. Blood. 2007; 109:130–8. [PubMed: 16940416]

35. Litvinov RI, Gorkun OV, Galanakis DK, Yakovlev S, Medved L, Shuman H, et al. Polymerization of fibrin: direct observation and quantification of individual B: b knob-hole interactions. Blood. 2007; 109:130–8. [PubMed: 16940416]

36. Lewis SD, Shields PP, Shafer JA. Characterization of the Kinetic Pathway for Liberation of Fibrinopeptides during Assembly of Fibrin. Journal of Biological Chemistry. 1985; 260:192–9.

Author Manuscript Author Manuscript Author Manuscript Author Manuscript

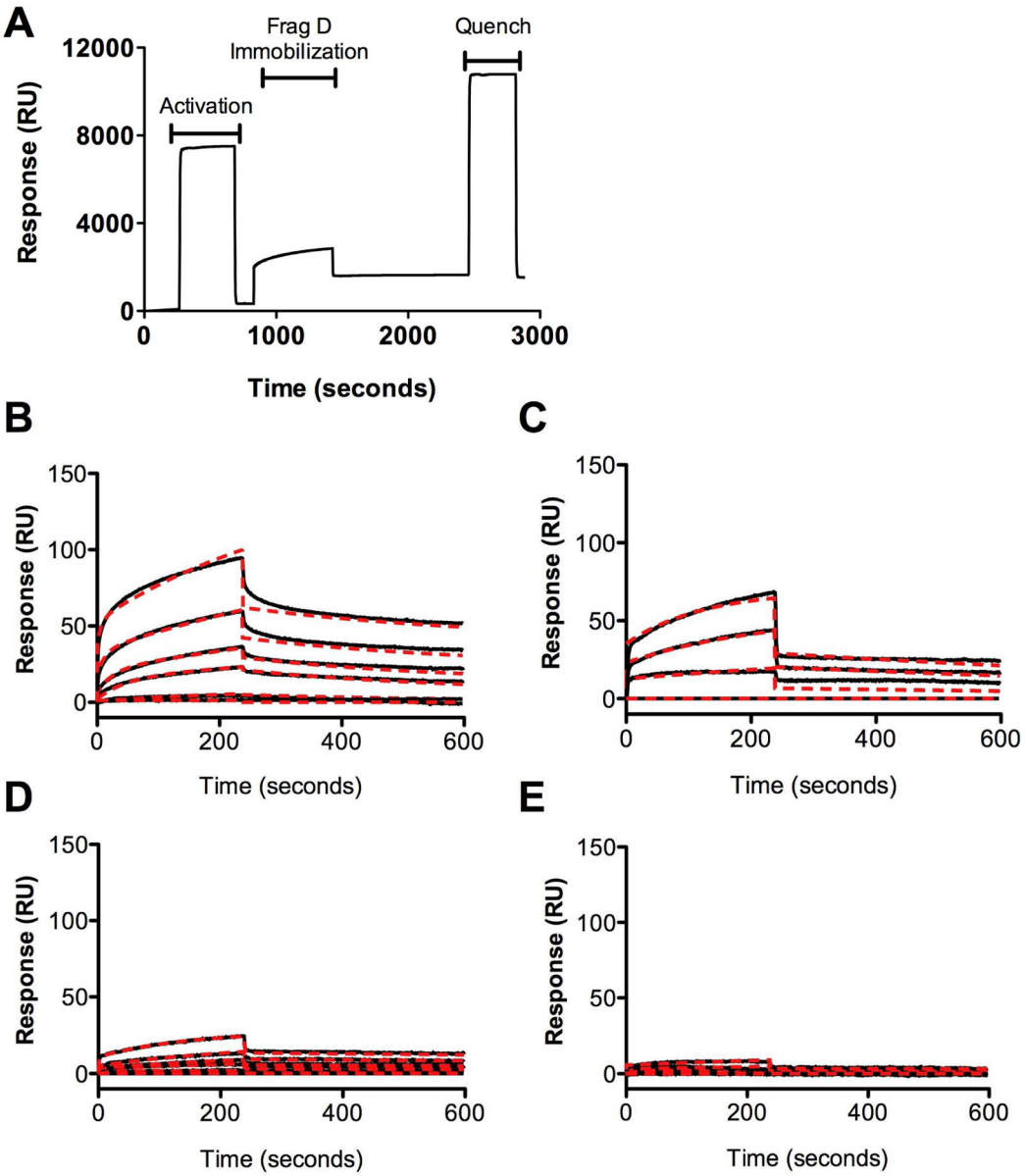

Figure 1. Experimental SPR curves and fits

Fragment D immobilization and analysis of binding capacity of knobs. Fragment D was immobilized on the surface of a sensorchip (A). The binding capacities of *knob B* peptide, AHRPYAAC (B), non-binding peptide, GPSPFPAC (C), and their respective PEGylated peptides (D, E) to fragment D were analyzed through SPR. Representative experimental binding curves and fits are shown in black and red, respectively.

Author Manuscript Author Manuscript Author Manuscript Author Manuscript

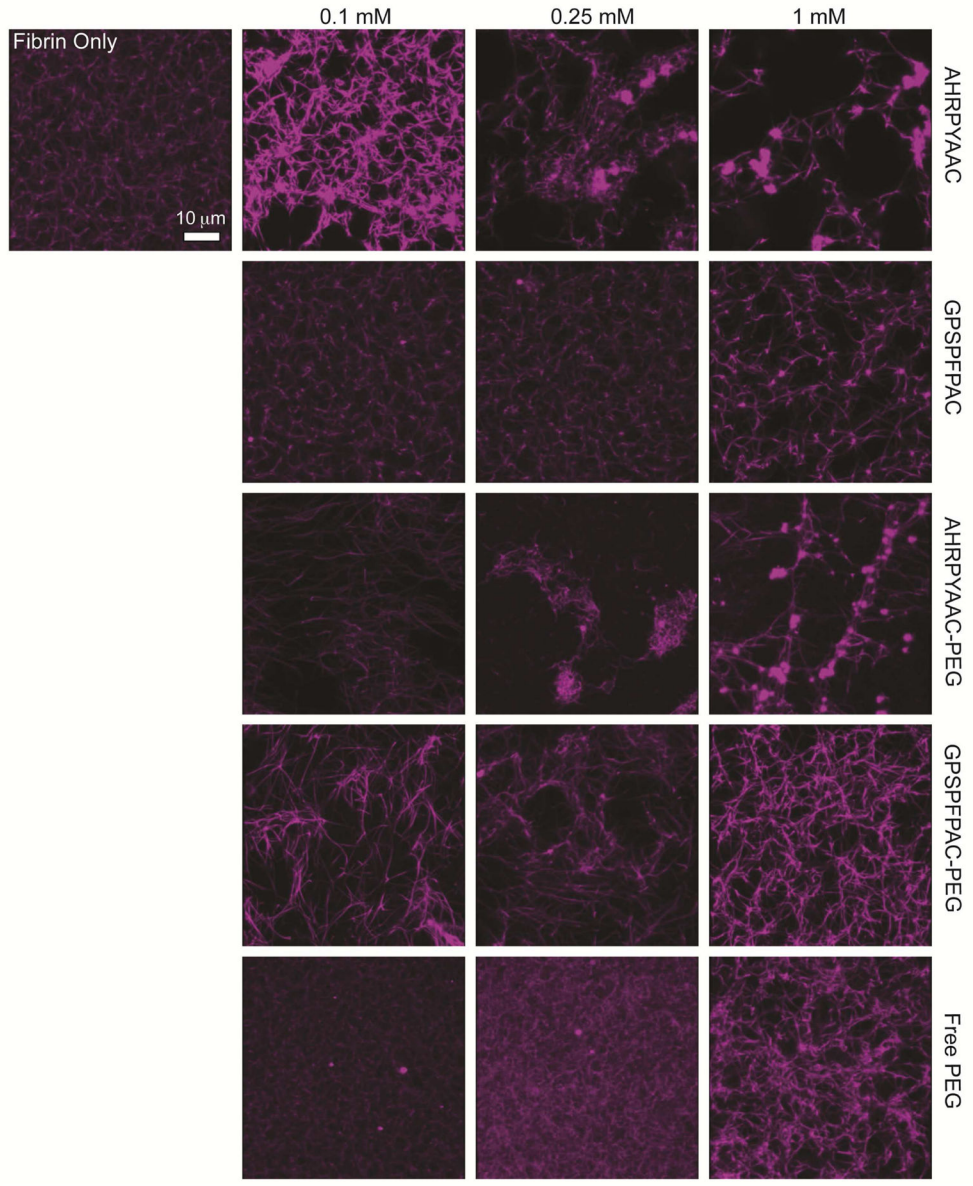

Figure 2. Incorporation of free or PEGylated knob B peptides grossly alters clot structure in a concentration dependent manner

Fibrin clots were formed in the presence of 0.1, 0.25 or 1 mM free or PEGylated *knob B*, negative control peptides or free PEG. The presence of free or PEGylated *knob B* peptides greatly alters fibrin network structure, resulting in thicker fibers and an increased porosity in a concentration dependent manner.

Author Manuscript Author Manuscript Author Manuscript Author Manuscript

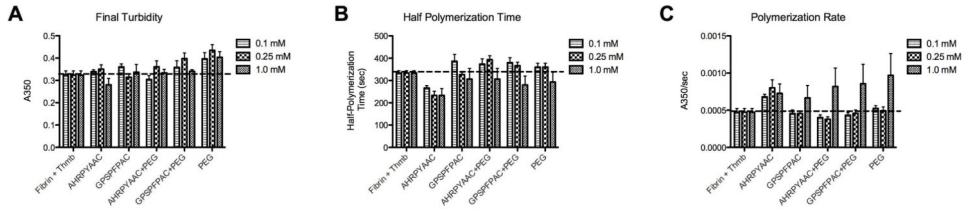

Figure 3. Quantitative analysis of polymerization dynamics

Turbidity curves obtained from clots formed in the presence of free or PEGylated *knob B*, negative control peptides or free PEG were analyzed to determine final clot turbidity (**A**), half polymerization time (**B**) and polymerization rate (**C**). Dotted lines indicate values obtained from fibrinogen + thrombin control samples. All concentrations of free *knob B* peptide tested increase rate of fibrin polymerization.

Author Manuscript Author Manuscript Author Manuscript Author Manuscript

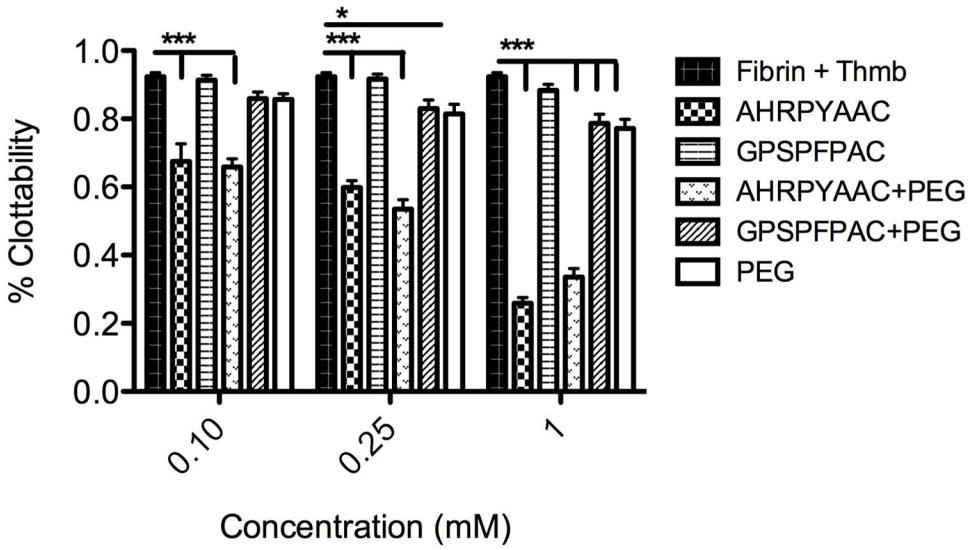

Figure 4. Incorporation of free or PEGylated knob B peptides inhibits protein incorporation into clot

Fibrin clots were formed in the presence of 1, 0.25 or 0.1 mM free or PEGylated *knob B* or negative control peptides or free PEG. Following completion of polymerization, percent clottable protein was determined by analyzing total protein in the clot liquor. The presence of either free or PEGylated *knob B* peptide significantly decreased percent clottability in a dose dependent manner compared to the fibrin only control. ***, $p<0.001$, *, $p<0.05$, relative to fibrinogen + thrombin control

Author Manuscript Author Manuscript Author Manuscript Author Manuscript

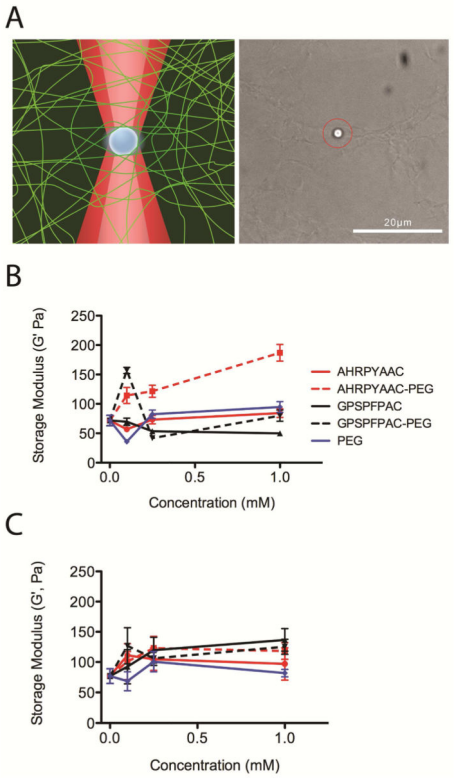

Figure 5. Analysis of microscale and bulk mechanical properties

Fibrin clots were formed in the presence of 0.1, 0.25 or 1 mM free or PEGylated *knob B* or negative control peptides or free PEG and then storage modulus (G′) was determined through AMR (schematic A; results B) or bulk cone and plate rheology (C). An illustration of a laser trapped bead embedded in the fibrin network and oscillated by laser tweezers (left) with the response of the bead detected by a second laser and a brightfield image (right) shown in A. AMR demonstrated a dose dependent increase in G′ in the presence of PEGylated *knob B* compared to control clots, while bulk analysis was not able to resolve significant differences in any conditions analyzed.

Author Manuscript Author Manuscript Author Manuscript Author Manuscript

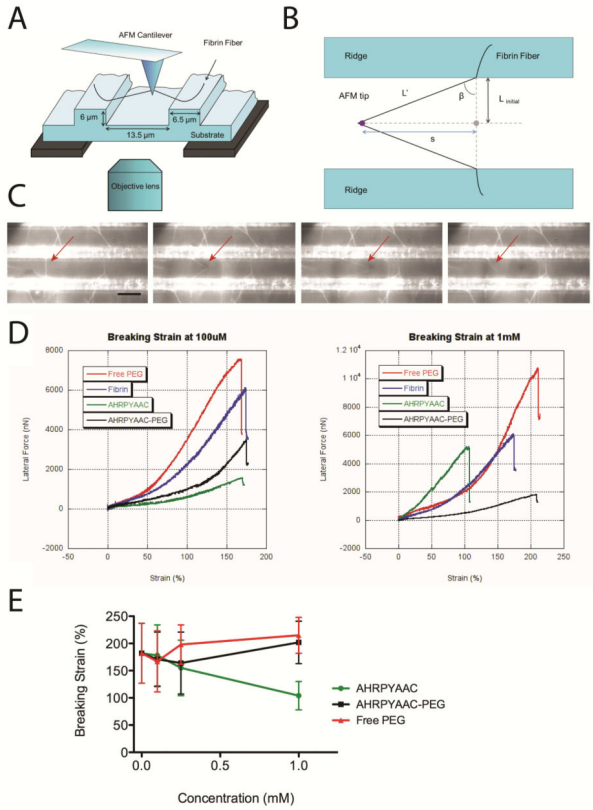

Figure 6. Single Fiber Manipulation for Determination of Breaking Strain

The fibrin fiber is suspended over the grooves of the striated substrate. The AFM cantilever tip, located above the sample, pulls on an individual fiber while the optical microscope, located below the sample, records fluorescent images of the manipulation (A). Top view of fiber manipulation (B). $L_{initial}$ is the initial length of the fiber, L′ is the stretched length of the fiber, and s is the distance the cantilever tip has traveled. L′ can be calculated trigonometrically using s and $L_{initial}$. Fluorescent microscopy movie frames showing a single fibrin fiber being stretched and broken (C). The individual fiber is indicated by the arrow. Scale bar is 15µm. This setup was utilized to analyze single fibrin fibers formed with the addition of various concentrations of AHRPYAAC, AHRPYAAC-PEG, and free PEG. Fibers were pulled until they broke. Single fiber extensibility is shown in D. Representative data showing the difference in breaking strain for single fiber manipulations of AHRPYAAC (green), AHRPYAAC-PEG (black), and Free PEG (red) at a concentration of 1mM or 100 µM. Note that the Fibrin concentration was held constant throughout all experiments and has been shown on and as a reference point. Fiber breaking strain is shown in (E). Numbers are given as a percentage of the fiber's original length. Normal, unmodified fibrin fiber breaking strain is given as a reference point.